Dynamic simulations
of Integrated Couped Cavity Lasers

P. Bardella[1]*, W.W. Chow[2], I. Montrosset[1]

1 Dipartimento di Elettronica e Telecomunicazioni, Politecnico di Torino, Torino, Italy
2 Sandia National Laboratories, Albuquerque, NM 87185, USA
*paolo.bardella@polito.it

Abstract—**We propose a general procedure that we used for the design of semiconductor integrated coupled cavity lasers taking advantage of the Photon-Photon Resonance effect to increase their direct modulation bandwidth. The procedure, based on an analysis at threshold of the longitudinal complete cavity modes, is combined with dynamic simulations of the lasers small and large signal modulations. As an example, we report the study of the bandwidth extension in two mutually coupled cavity DBR lasers.**

Keywords—component; semiconductor laser, modulation bandwidth, Photon-Photon Resonance, Coupled Cavities

I. INTRODUCTION

The continuously increasing demand of optical source for high speed communication is driving an incessant research for directly modulated semiconductor lasers with large modulation bandwidth. Many solutions have been proposed to enhance the direct modulation bandwidth of edge emitting semiconductor lasers, which is generally limited by the intra-cavity interaction between carriers and photons (CPR, carrier-photon resonance).

An extension of the -3dB small signal modulation frequency (f_{-3dB}) can be obtained taking advantage of the "detuned loading effect" which occurs when the lasing mode is placed at a frequency slightly lower with respect to the minimum threshold condition. This technique has been used in DBR [1] and DFB lasers [2] and in coupled passive cavities [3]; however, the f_{-3dB} improvement is generally by 20% at the most. Larger bandwidth extensions have been obtained by external injection locking of a slave laser to a master optical source [4] or between coupled vertical-cavity surface-emitting lasers [5].

Finally, the Photon-Photon Resonance effect (relaying on the carrier-sustained interaction between the lasing mode and its closes longitudinal non-lasing one) may allow a significant extensions of f_{-3dB}, well beyond the limit of the CPR. Although this effect has been successfully used also to extend the modulation bandwidth of DBR laser [6], it has been widely used in lasers with coupled cavities, such as Complex Cavity Injection Grating [7], DFB with Integrated Feedback [8], Integrated Coupled Cavity (ICC) [9] and single-mode cavity with feedback effects [10].

When relying on the PPR effect, a careful design of the laser cavity and an accurate choice of the material parameters is required for the device to operate in the desired conditions. In particular, the terminal facets reflectivities and the lengths and grating coupling coefficients of the different section of the laser have to be properly chosen to ensure that the frequency separa-
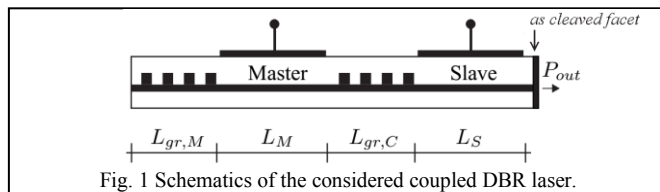

Fig. 1 Schematics of the considered coupled DBR laser.

tion between the two interacting modes (f_{PPR}) is compatible with the desired f_{-3dB}. For this reason, we propose here a simple yet powerful design strategy, based on an analysis of the cavity modes separation at the laser threshold validated trough dynamic simulations above threshold. This approach is very general and can be applied, albeit with some variations, to all the previously cited laser devices exploiting the PPR effect; however, for the sake of simplicity, we will focus here on the ICC laser similar to the device proposed in [9], consisting of two integrated mutually coupled cavity DBR lasers (Fig.1). We will address additional devices during the presentation.

II. CAVITY MODES ANALYSIS

We evaluate, at threshold, the round trip gain (RTG) and phase vs. frequency of the lasing mode and the adjacent ones. We compute these quantities with a transmission matrix approach, calculating the left and right complex reflectivities respect to a chosen reference plane in the laser cavity [11]. We present in Fig. 2a-c examples of the obtained results for three perturbations of the optical length corresponding to a phase shift δφ: these small variations can be generally controlled either thermally or electrically. Examples of corresponding small signal modulation responses (SSMRs) are presented in Fig. 2d.
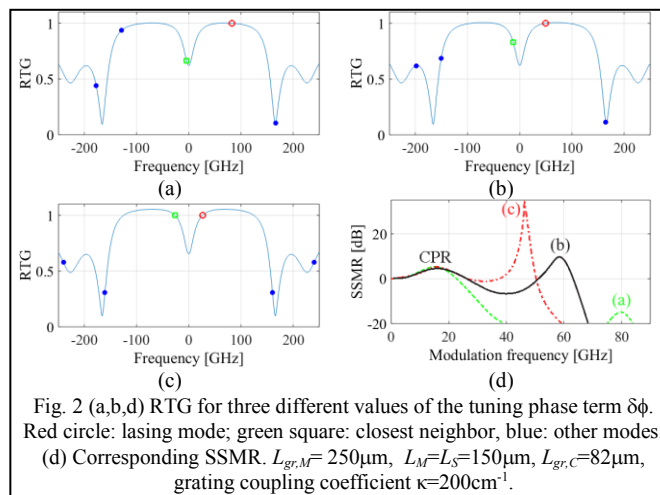

Fig. 2 (a,b,d) RTG for three different values of the tuning phase term δφ. Red circle: lasing mode; green square: closest neighbor, blue: other modes. (d) Corresponding SSMR. $L_{gr,M}$= 250μm, L_M=L_S=150μm, $L_{gr,C}$=82μm, grating coupling coefficient κ=200cm⁻¹.

11

In Fig. 2a, the interaction between the lasing mode and its closest one is very weak, due to their huge frequency separation and to the large difference of their RTGs. The typical SSMR is limited by the CPR (Fig. 2d, dashed line) and the PPR peak, appearing around 80GHz, is too weak to fill the gap with the CPR peak: as a result, the -3dB bandwidth is not enhanced. Increasing $\delta\phi$, the interaction between the lasing mode and the nearest one becomes more effective; when the RTG of the non-lasing closest mode is approximately 0.8 (Fig. 2b), the SSMR is expected to show an improvement of the -3dB bandwidth (Fig. 2d, continuous line). This particular condition only occurs for a limited range of $\delta\phi$. Indeed, if $\delta\phi$ increases further, two modes tends to the condition RTG=1 (Fig. 2c); in the SSMR we observe a pronounced peak (Fig. 2d, dashed-dotted line) at a frequency corresponding to f_{PPR}, which indicates that the device is presenting self-sustained relaxation oscillations [SS-RO].

Thanks to these considerations, we are able to determine if, for an assigned set of device cavity parameters, an extension of the modulation bandwidth occurs and to have an indication of the achievable f_{-3dB}.

III. Dynamic Simulation results

Once we have found a set of parameters fulfilling the required f_{PPR}, we perform simulations based on a 1D Finite Difference Time Domain model (FDTW) [13] to calculate the small and large signal modulations responses of the laser. We use these simulations to validate the design procedure and to identify the influence on the PPR of the material physical parameters, in particular differential gain, linewidth enhancement factor α_{LEF}, and gain compression factor ε.

A map of the SSMR, having on the abscissae the modulation frequency and on the ordinates the phase change $\delta\phi$ introduced in the Slave section to tune the position of the cavity modes, allows to easily determine if the modulation bandwidth is really extended and if it sufficiently flat. An example is shown in Fig. 3, for a set of cavity parameters chosen to obtain
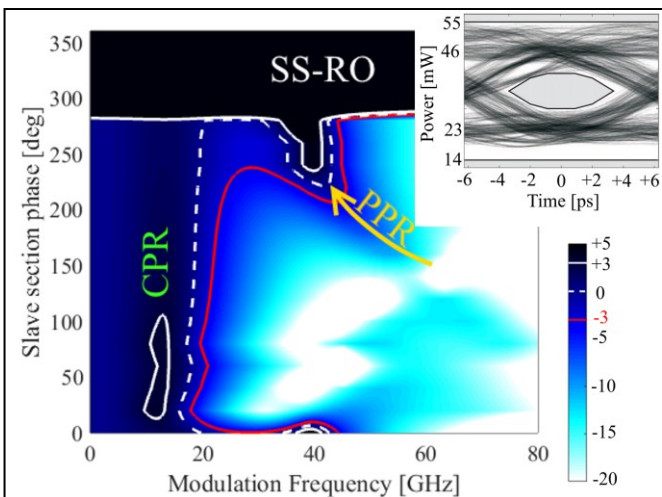

Fig. 3 SSMR map, in dB, calculated with the FDTW. The contour lines indicate the -3dB (continuous red), 0dB (dashed white) and +3dB (continuous white) levels. The injected currents are 8mA (master) and 60mA (slave), resulting in 25mW output power. Inset: eye diagram calculated with a Non-Return-To-Zero random sequence with an 80GHz bit rate for a 250º phase.

f_{PPR}=40GHz ($L_{gr,M}$=250µm, L_M=L_S=200µm, $L_{gr,C}$=82µm, κ=100cm^{-1}), ε=5×10^{-17} cm^3, α_{LEF}=3 [12]. For 0≤$\delta\phi$≤150°, the CPR dominates the response, while for larger values of $\delta\phi$ the PPR effect, indicated by the arrow in Fig. 3, becomes evident. When $\delta\phi$=250°, f_{-3dB}=45GHz, with the PPR peak at 40 GHz as designed, and the eye diagram is still open when the laser is modulated at a repetition frequency as high as 80Gbit/s (inset in Fig. 3). Finally, in the upper part of the map, the dark horizontal strips represents a region of SSRO [12].

To investigate the sensitivity of the modulation response maps to the material parameters, we varied the gain saturation from ε=2×10^{-17}cm^3 to ε=8×10^{-17}cm^3 (Fig. 4). We observed a significant reduction of the CPR peak when increasing ε, but the position of the PPR peak is unchanged. The effect of the variation of the linewidth enhancement factor is more significant, indicating how the PPR effect is sensitive to the variation of material refractive index. The area of SS-RO, increased with α_{LEF} (α_{LEF}=5, Fig.5b), decreases reducing this parameter (α_{LEF}=2, Fig. 5a), finally disappearing when α_{LEF}=1.

We used successfully this procedure to design and to analyze all the complex cavity lasers based on the PPR effect.
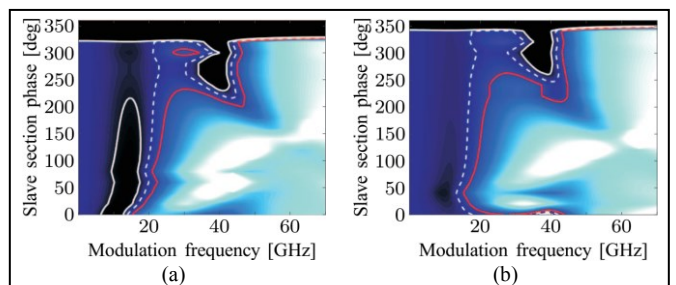

Fig. 4 SSMR map for the case in Fig. 8 with ε=2×10^{-17} cm^3 and ε=8×10^{-17} cm^3 in (a) and (b), respectively. Notations as in Fig. 3.
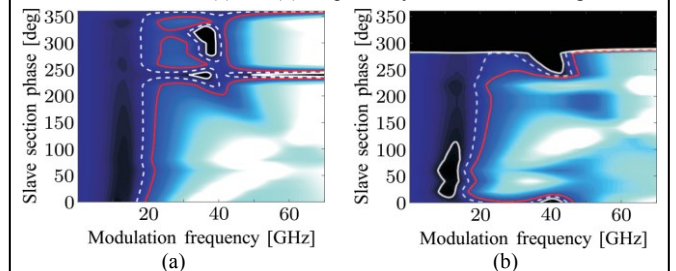

Fig. 5 SSMR map for the case in Fig. 8 with α_{LEF} =2 and α_{LEF} =4 in (a) and (b), respectively. Notations as in Fig. 3.

References

[1] I. Montrosset at al., SPIE Proceedings, vol. 9134, May 2014
[2] U. Feiste, IEEE J. Quantum Electron., vol. 34, Dec. 1998
[3] X. Pan et al., IEEE J. Quantum Electron., vol 25, Jun. 1989
[4] K. Vahala et al. Applied Physics Letters, vol. 45, no. 5, 1984
[5] E. Lau et al., IEEE J. Select. Top. Q. Electron., vol. 15, May 2009
[6] Dalir H., Applied Physics Express, vol. 7, n. 25, Jan 2014
[7] P. Bardella et al., IEEE J. Select. Top. Q. Electron., vol.19, Jul. 2013
[8] M. Vallone et al., IEEE J. Quantum Electron., vol.47, Oct. 2011
[9] M. Radziunas et al., IEEE J. Select. Top. Q. Electron., vol. 13, Jan. 2007
[10] A. Tauke-Pedretti et al., IEEE Photonics Technol. Lett., vol. 23, 2011
[11] F. Grillot et al., IEEE J. Select. Top. Q. Electron., vol. 19, Jul. 2013
[12] P. Bardella et al., *Photonics* , vol. 3, no. 1, 2016
[13] P. Bardella et al., IEEE J. Select. Top. Q. Electron., vol. 11, Mar. 2005